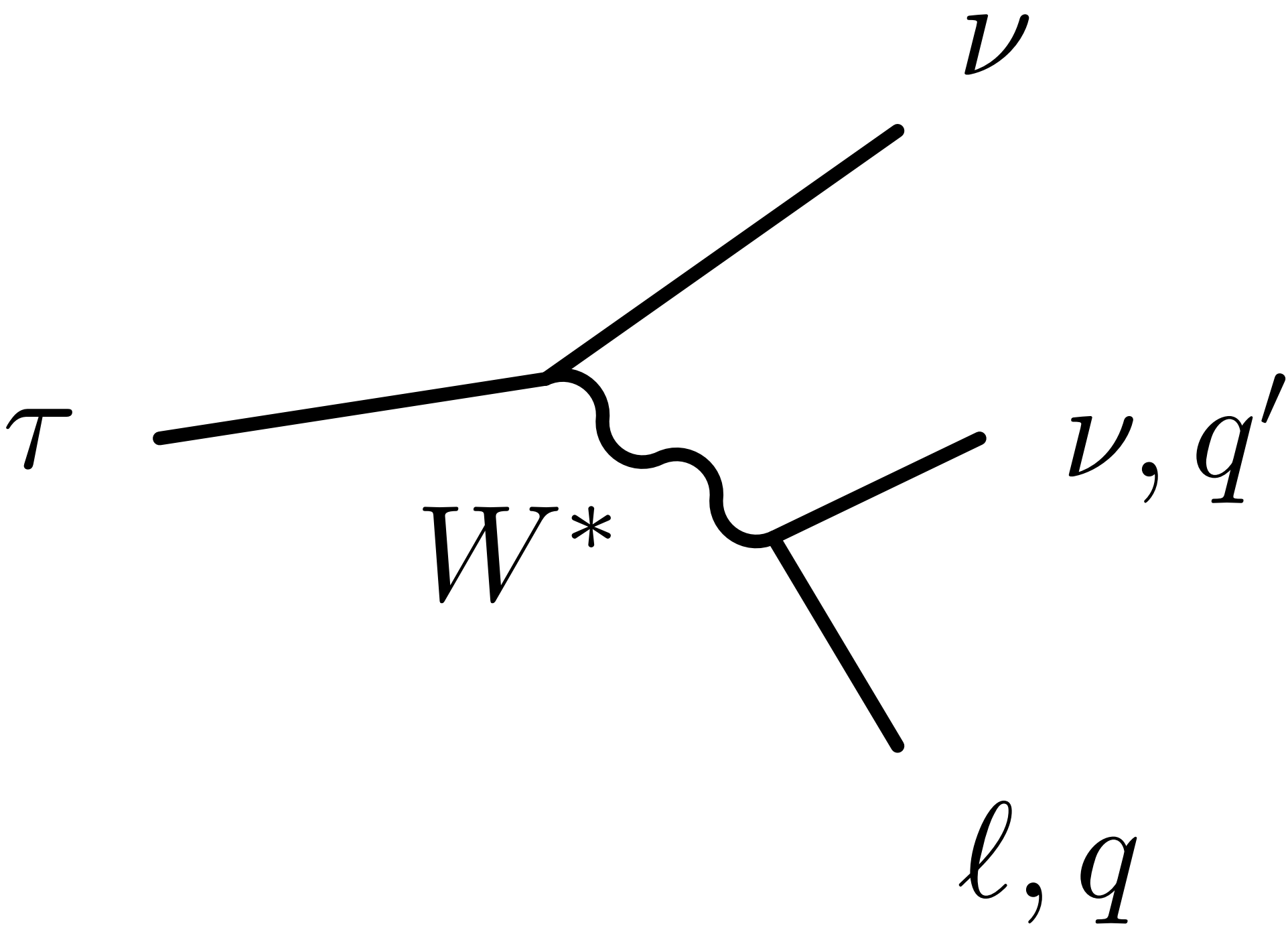
ν
τ
ν, q'
W^*
ℓ, q

February 2008
LPTHE-07-03

The anti-k_t jet clustering algorithm

Matteo Cacciari and Gavin P. Salam
LPTHE
UPMC Université Paris 6,
Université Paris Diderot – Paris 7,
CNRS UMR 7589, Paris, France

Gregory Soyez
Brookhaven National Laboratory, Upton, NY, USA

Abstract: The k_t and Cambridge/Aachen inclusive jet finding algorithms for hadron-hadron collisions can be seen as belonging to a broader class of sequential recombination jet algorithms, parametrised by the power of the energy scale in the distance measure. We examine some properties of a new member of this class, for which the power is negative. This "anti-k_t" algorithm essentially behaves like an idealised cone algorithm, in that jets with only soft fragmentation are conical, active and passive areas are equal, the area anomalous dimensions are zero, the non-global logarithms are those of a rigid boundary and the Milan factor is universal. None of these properties hold for existing sequential recombination algorithms, nor for cone algorithms with split–merge steps, such as SISCone. They are however the identifying characteristics of the collinear unsafe plain "iterative cone" algorithm, for which the anti-k_t algorithm provides a natural, fast, infrared and collinear safe replacement.

1 Introduction and definition

Jet clustering algorithms are among the main tools for analysing data from hadronic collisions. Their widespread use at the Tevatron and the prospect of unprecedented final-state complexity at the upcoming Large Hadron Collider (LHC) have stimulated considerable debate concerning the merits of different kinds of jet algorithm. Part of the discussion has centred on the relative advantages of sequential recombination (k_t [1] and Cambridge/Aachen [2]) and cone (e.g. [3]) jet algorithms, with an issue of particular interest being that of the regularity of the boundaries of the resulting jets. This is related to the question of their sensitivity to non-perturbative effects like hadronisation and underlying event contamination and arises also in the context of experimental calibration.

Recently [4], tools have been developed that allow one, for the first time, to support the debate with analytical calculations of the contrasting properties of boundaries of jets within different algorithms. One of the main results of that work is that all known infrared and collinear (IRC) safe algorithms have the property that soft radiation can provoke irregularities in the boundaries of the final jets. This is the case even for SISCone [5], an IRC-safe jet algorithm based on the search for stable cones, together with a split–merge step that disentangles overlapping stable cones. One might describe current IRC-safe algorithms in general as having a 'soft-adaptable' boundary.

A priori it is not clear whether it is better to have regular ('soft-resilient') or less regular (soft-adaptable) jets. In particular, regularity implies a certain rigidity in the jet algorithm's ability to adapt a jet to the successive branching nature of QCD radiation. On the other hand knowledge of the typical shape of jets is often quoted as facilitating experimental calibration of jets, and soft-resilience can simplify certain theoretical calculations, as well as eliminate some parts of the momentum-resolution loss caused by underlying-event and pileup contamination.

Examples of jet algorithms with a soft-resilient boundary are the plain "iterative cone" algorithm, as used for example in the CMS collaboration [6], and fixed-cone algorithms such as Pythia's [7] CellJet. The CMS iterative cone takes the hardest object (particle, calorimeter tower) in the event, uses it to seed an iterative process of looking for a stable cone, which is then called a jet. It then removes all the particles contained in that jet from the event and repeats the procedure with the hardest available remaining seed, again and again until no seeds remain. The fixed-cone algorithms are similar, but simply define a jet as the cone around the hardest seed, skipping the iterative search for a stable cone. Though simple experimentally, both kinds of algorithm have the crucial drawback that if applied at particle level they are collinear unsafe, since the hardest particle is easily changed by a quasi-collinear splitting, leading to divergences in higher-order perturbative calculations.[1]

In this paper it is not our intention to advocate one or other type of algorithm in the debate concerning soft-resilient versus soft-adaptable algorithms. Rather, we feel that this debate can be more fruitfully served by proposing a simple, IRC safe, soft-resilient jet algorithm, one that leads to jets whose shape is not influenced by soft radiation. To do so, we take a quite non-obvious route, because instead of making use of the concept of a stable cone, we start by generalising the existing sequential recombination algorithms, k_t [1] and Cambridge/Aachen [2].

As usual, one introduces distances d_{ij} between entities (particles, pseudojets) i and j and d_{iB} between entity i and the beam (B). The (inclusive) clustering proceeds by identifying the smallest of the distances and if it is a d_{ij} recombining entities i and j, while if it is d_{iB} calling i a jet and removing it from the list of entities. The distances are recalculated and the procedure repeated until no entities are left.

The extension relative to the k_t and Cambridge/Aachen algorithms lies in our definition of the distance measures:

$$d_{ij} = \min(k_{ti}^{2p}, k_{tj}^{2p}) \frac{\Delta_{ij}^2}{R^2}\,, \tag{1a}$$

$$d_{iB} = k_{ti}^{2p}\,, \tag{1b}$$

where $\Delta_{ij}^2 = (y_i - y_j)^2 + (\phi_i - \phi_j)^2$ and k_{ti}, y_i and ϕ_i are respectively the transverse momentum, rapidity and azimuth of particle i. In addition to the usual radius parameter R, we have added a parameter p to govern the relative power of the energy versus geometrical (Δ_{ij}) scales.

For $p = 1$ one recovers the inclusive k_t algorithm. It can be shown in general that for $p > 0$ the behaviour of the jet algorithm with respect to soft radiation is rather similar to that observed for the k_t algorithm, because what matters is the ordering between particles and for finite Δ this is maintained for all positive values of p. The case of $p = 0$ is special and it corresponds to the inclusive Cambridge/Aachen algorithm.

[1] This is discussed in the appendix in detail for the iterative cone, and there we also introduce the terminology iterative cone with split–merge steps (IC-SM) and iterative cone with progressive removal (IC-PR), so as to distinguish the two broad classes of iterative cone algorithms.

Negative values of p might at first sight seem pathological. We shall see that they are not.[2] The behaviour with respect to soft radiation will be similar for all $p < 0$, so here we will concentrate on $p = -1$, and refer to it as the "anti-k_t" jet-clustering algorithm.

2 Characteristics and properties

2.1 General behaviour

The functionality of the anti-k_t algorithm can be understood by considering an event with a few well-separated hard particles with transverse momenta k_{t1}, k_{t2}, ... and many soft particles. The $d_{1i} = \min(1/k_{t1}^2, 1/k_{ti}^2)\Delta_{1i}^2/R^2$ between a hard particle 1 and a soft particle i is exclusively determined by the transverse momentum of the hard particle and the Δ_{1i} separation. The d_{ij} between similarly separated soft particles will instead be much larger. Therefore soft particles will tend to cluster with hard ones long before they cluster among themselves. If a hard particle has no hard neighbours within a distance $2R$, then it will simply accumulate all the soft particles within a circle of radius R, resulting in a perfectly conical jet.

If another hard particle 2 is present such that $R < \Delta_{12} < 2R$ then there will be two hard jets. It is not possible for both to be perfectly conical. If $k_{t1} \gg k_{t2}$ then jet 1 will be conical and jet 2 will be partly conical, since it will miss the part overlapping with jet 1. Instead if $k_{t1} = k_{t2}$ neither jet will be conical and the overlapping part will simply be divided by a straight line equally between the two. For a general situation, $k_{t1} \sim k_{t2}$, both cones will be clipped, with the boundary b between them defined by $\Delta R_{1b}/k_{t1} = \Delta_{2b}/k_{t2}$.

Similarly one can work out what happens with $\Delta_{12} < R$. Here particles 1 and 2 will cluster to form a single jet. If $k_{t1} \gg k_{t2}$ then it will be a conical jet centred on k_1. For $k_{t1} \sim k_{t2}$ the shape will instead be more complex, being the union of cones (radius $< R$) around each hard particle plus a cone (of radius R) centred on the final jet.

The key feature above is that the soft particles do not modify the shape of the jet, while hard particles do. I.e. the jet boundary in this algorithm is resilient with respect to soft radiation, but flexible with respect to hard radiation.[3]

The behaviours of different jet algorithms are illustrated in fig. 1. We have taken a parton-level event together with $\sim 10^4$ random soft 'ghost' particles (as in [4]) and then clustered them with 4 different jet algorithms. For each of the partonic jets, we have shown the region within which the random ghosts are clustered into that jet. For the k_t and Cambridge/Aachen algorithms, that region depends somewhat on the specific set of ghosts and the jagged borders of the jets are a consequence of the randomness of the ghosts — the jet algorithm is adaptive in its response to soft particles, and that adaptiveness applies also to the ghosts which take part in the clustering. For SISCone one sees that single-particle jets are regular (though with a radius $R/2$ — as pointed out in [4]), while composite jets have more varied shapes. Finally with the anti-k_t algorithm, the hard jets are all circular with a radius R, and only the softer jets have more complex shapes. The pair of jets near $\phi = 5$ and $y = 2$ provides an interesting example in this respect. The left-hand one is much softer than the right-hand one. SISCone (and Cam/Aachen) place the boundary between

[2] Note that, for $p < 0$, $\min(k_{ti}^{2p}, k_{tj}^{2p})$ differs from another possible extension, $[\min(k_{ti}^2, k_{tj}^2)]^p$, which *can* lead to strange behaviours.

[3] For comparison, IC-PR algorithms behave as follows: with $R < \Delta_{12} < 2R$, the harder of the two jets will be fully conical, while the softer will be clipped regardless of whether p_{t1} and p_{t2} are similar or disparate scales; with $\Delta_{12} < R$ the jet will be just a circle centred on the final jet.

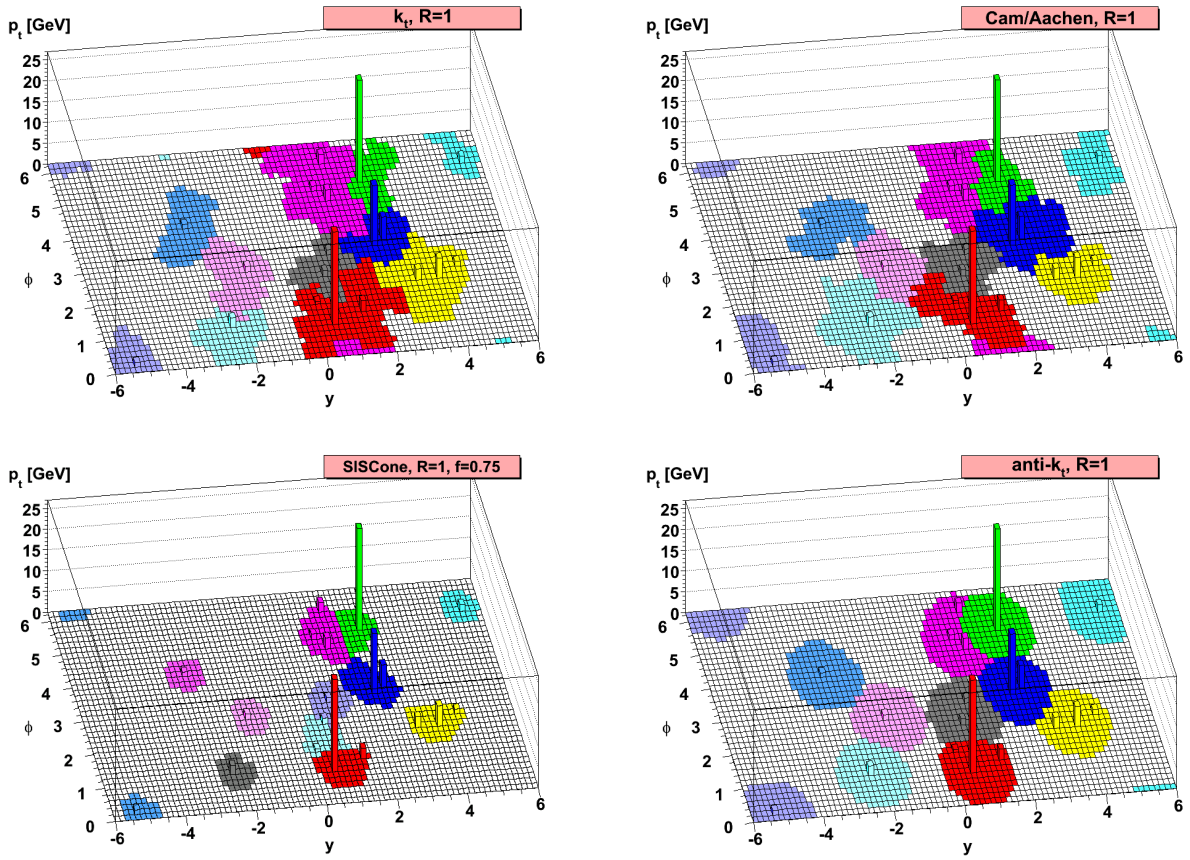

Figure 1: A sample parton-level event (generated with Herwig [8]), together with many random soft "ghosts", clustered with four different jets algorithms, illustrating the "active" catchment areas of the resulting hard jets. For k_t and Cam/Aachen the detailed shapes are in part determined by the specific set of ghosts used, and change when the ghosts are modified.

the jets roughly midway between them. Anti-k_t instead generates a circular hard jet, which clips a lens-shaped region out of the soft one, leaving behind a crescent.

The above properties of the anti-k_t algorithm translate into concrete results for various quantitative properties of jets, as we outline below.

2.2 Area-related properties

The most concrete context in which to quantitatively discuss the properties of jet boundaries for different algorithms is in the calculation of jet areas.

Two definitions were given for jet areas in [4]: the passive area (a) which measures a jet's susceptibility to point-like radiation, and the active area (A) which measures its susceptibility to diffuse radiation. The simplest place to observe the impact of soft resilience is in the passive area for a jet consisting of a hard particle p_1 and a soft one p_2, separated by a $y-\phi$ distance Δ_{12}. In usual IRC safe jet algorithms (JA), the passive area $a_{\mathrm{JA},R}(\Delta_{12})$ is πR^2 when $\Delta_{12}=0$, but changes when Δ_{12} is increased. In contrast, since the boundaries of anti-k_t jets are unaffected by soft radiation,

	a(1PJ)	A(1PJ)	σ(1PJ)	Σ(1PJ)	d	D	s	S
k_t	1	0.81	0	0.28	0.56	0.52	0.45	0.41
Cam/Aachen	1	0.81	0	0.26	0.08	0.08	0.24	0.19
SISCone	1	1/4	0	0	-0.06	0.12	0.09	0.07
anti-k_t	1	1	0	0	0	0	0	0

Table 1: A summary of main area results for the anti-k_t algorithm compared to those for other IRC safe algorithms in [4]: the passive (a) and active (A) areas for 1-particle jets (1PJ), the magnitude of the passive/active area fluctuations (σ, Σ), followed by the coefficients of the respective anomalous dimensions (d, D; s, S), in the presence of perturbative QCD radiation. All results are normalised to πR^2, and rounded to two decimal figures. For algorithms other than anti-k_t, active-area results hold only in the small-R limit, though finite-R corrections are small.

their passive area is always independent of Δ_{12}:

$$a_{\text{anti-}k_t,R}(\Delta_{12}) = \pi R^2 \,. \tag{2}$$

Furthermore, since soft particles only cluster among themselves *after* all clusterings with hard particles have occurred, passive and active areas are identical, another feature that is unique to the anti-k_t algorithm. Thus, specifically for our energy-ordered two-particle configuration, the active area is

$$A_{\text{anti-}k_t,R}(\Delta_{12}) = a_{\text{anti-}k_t,R}(\Delta_{12}) = \pi R^2 \,. \tag{3}$$

In [4] the fact that $a_{\text{JA},R}(0) \neq a_{\text{JA},R}(\Delta_{12})$ (and similarly for the active area) meant that the jet areas acquired an anomalous dimension in their dependence on the jet transverse momentum p_{tJ}, related to emission of perturbative soft particles:

$$\langle a_{\text{JA},R} \rangle = \pi R^2 + d_{\text{JA},R} \frac{C_1}{\pi b_0} \ln \frac{\alpha_s(Q_0)}{\alpha_s(R p_{tJ})} \,, \tag{4}$$

where C_1 is the colour factor of the hard particle in the jet, Q_0 is the non-perturbative scale and the coefficient of the anomalous dimension, $d_{\text{JA},R}$, is given by

$$d_{\text{JA},R} = \int_0^{2R} \frac{d\theta}{\theta} (a_{\text{JA},R}(\theta) - \pi R^2) \,. \tag{5}$$

Obviously in this case $d_{\text{anti-}k_t,R} = 0$ and similarly for the active area anomalous dimension coefficient $D_{\text{anti-}k_t,R}$. One corollary of this is that anti-k_t jet areas can be calculated perturbatively, order by order, since they are infrared safe. In this respect we recall that they do deviate from πR^2 for configurations with several neighbouring hard particles.

A summary of these and other properties of the jet area is given in table 1, together with a comparison to other IRC safe algorithms as studied in [4]. Fig. 2 illustrates the distribution of areas in dijet events at the LHC (generated with Pythia 6.4, with a transverse momentum cut of 1 TeV on the $2 \to 2$ scattering, considering those among the two hardest jets in each event that have $|y| < 2$), compared with those for other algorithms, and one sees a near δ-function at an area of πR^2, to be compared to the broader distributions of other algorithms. Fig. 3 shows the mean jet area, together with a band representing the event-by-event fluctuations of the area, as a function of the jet p_t in $gg \to gg$ events, now generated with Herwig. This highlights the independence of the area on the jet p_t and, once again, the very small fluctuations in the jet area. In this respect, we recall that the impact of the UE and pileup on the momentum resolution for jets is related both to the typical value of the area (smaller than k_t, similar to Cambridge/Aachen, larger than SISCone) and to the extent of the fluctuations of the area, which are close to zero only for anti-k_t.

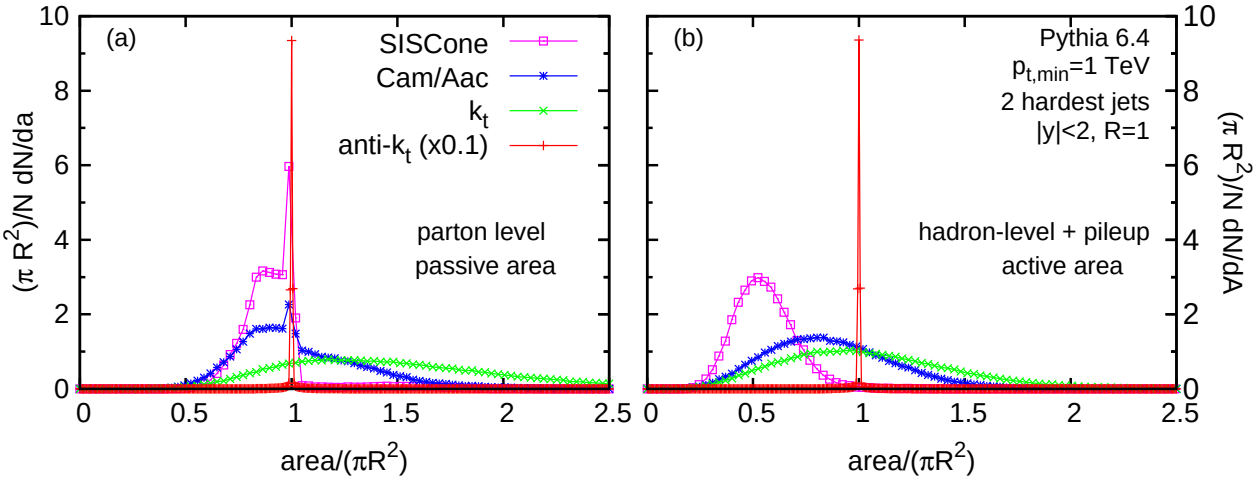

Figure 2: Distribution of areas in dijet events at the LHC. We have generated events with Pythia 6.4 with a $p_{t,min}$ of 1 TeV. Only the two hardest jets have been kept with a further requirement $|y| \leq 2$. The area distribution obtained from anti-k_t (scaled by 0.1) is compared to the other algorithms. (a) passive area at parton level; (b) active area at hadron level including the underlying event and pileup corresponding to high luminosity LHC running.

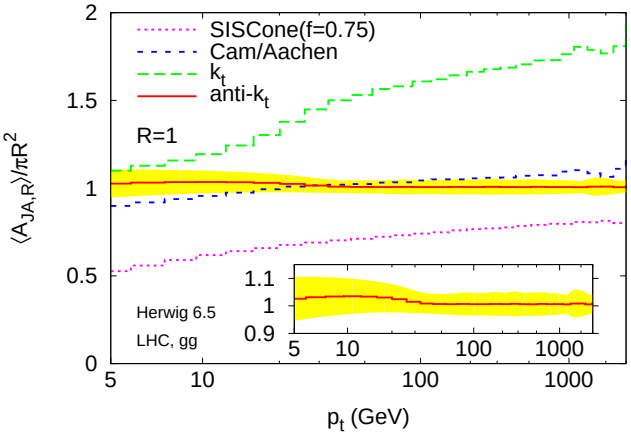

Figure 3: Average jet area in dijet events at the LHC. We have generated events with Herwig 6.5 and only the two hardest jets with $|y| \leq 2$ have been kept. The curves correspond to the average jet area at a given p_t. The yellow band around the anti-k_t line corresponds to the area fluctuations. For clarity, the latter are not shown for the other algorithms. The encapsulated graph is a zoom on the anti-k_t results. Note that the horizontal scale is $\ln\ln(p_t/\Lambda_{QCD})$ with $\Lambda_{QCD} = 200$ MeV.

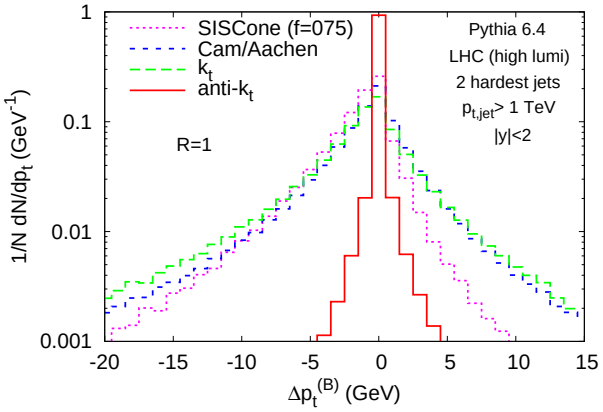

Figure 4: Distribution of back-reaction for the anti-k_t algorithm as compared to k_t, Cambridge/Aachen and SISCone. It is calculated for dijet events simulated with Pythia 6.4 in which the two hardest jets have $p_t > 200\,\text{GeV}$ and are both situated at $|y| < 2$. The back reaction corresponds to the net transverse momentum change of each of the two hardest jets due to the reassignment of non-pileup particles when one adds high-luminosity LHC pileup to the event (~ 25 pp interactions per bunch crossing).

Back reaction. Suppose one has a hard scattering event that leads to a set of jets $\{J_i\}$. If one adds a soft event (UE, pileup) to it and reruns the the algorithm, one will obtain a set of jets $\{\tilde{J}_i\}$ that differ in two respects: soft energy will have been added to each jet, and additionally the way the particles from the hard event are distributed into jets may also have changed: even if one finds the $\tilde{J}_i$ that is closest to the original J_1, the two jets will not contain exactly the same subset of particles from the original hard event. This was called "back-reaction" in [4]. If the soft particles that are added have a density ρ of transverse momentum per unit area, then for usual sequential recombination algorithms the probability, $dP/d\ln \Delta p_t^{(B)}$, of having a back reaction of $\Delta p_t^{(B)}$ is $\mathcal{O}\left(\alpha_s \rho/\Delta p_t^{(B)}\right)$ for $\Delta p_t^{(B)} \gtrsim \rho$.[4]

For the anti-k_t algorithm, one can show that the probability of back-reaction is suppressed not by the amount of back reaction itself, $\Delta p_t^{(B)}$, but by the jet transverse momentum p_{tJ}, leading to a much smaller effect. The impact of this is illustrated in fig. 4, which shows the back reaction that occurs for the hard jet events when adding high luminosity LHC pileup to the event. One sees that it is strongly suppressed for the anti-k_t algorithm relative to the others, a characteristic that can help reduce the smearing of jets' momenta due to the UE and pileup.

2.3 Other properties

Non-global logarithms. Resummations of observables involving boundaries in phase space are known to involve 'non-global' logarithms. Examples are the jet-mass distribution [9] and energy flow distributions in restricted regions [10, 11, 12]. In both cases there are all-order single logarithmic terms (for a hard scale Q, $\alpha_s^n \ln^n Q/m$ for jet-mass distributions, $\alpha_s^n \ln^n Q/E$ for energy flow), that are related to the impact of emissions outside the boundary that radiate a gluon across the boundary and so affect the observable defined only on particles within the boundary.

[4] For smaller values of $\Delta p_t^{(B)}$ the full answer requires a resummation that has yet to be carried out, and in the case of SISCone, it depends on the nature of the fluctuations of soft event.

It was pointed out in [13] that the structure of these non-global terms is more complex with clustering jet algorithms, because the boundary of the jet itself depends on the soft radiation.[5] Furthermore this affects even the contribution from independent emissions [14] which remained simple in the case of a rigid boundary. So far these effects have been calculated only for the k_t algorithm, while for the cone and Cambridge/Aachen algorithms little is known about the non-global logarithms other than that they too involve a subtle interaction between the clustering and the non-global resummation.

Because soft radiation does not affect the boundary of anti-k_t jets, it is straightforward to see that their single-logarithmic non-global terms are identically those associated with ideal cones, considerably simplifying their determination.

Milan factor. A crucial ingredient in analytical studies of non-perturbative effects in event and jet-shapes is the Milan factor [15, 16, 17], which is the correction that relates calculations made in a single soft (almost non-perturbative) gluon approximation to calculations in which the soft gluon splits at large angle. A remarkable characteristic of the Milan factor ('universality') is that it is identical for all event shapes. This is essentially because for all event shapes, if one takes an event with hard momenta p_i and soft momenta k_i, then the event shape can be approximated as

$$V(\{p_i\},\{k_i\}) = V(\{p_i\}) + \sum_{\{k_i\}} f_V(\theta_i,\{p_i\})k_{ti} \tag{6}$$

where f_V is a function specific to the event shape observable V. The key feature is the linearity of the second term on the right-hand side of eq. (6) (see also [18]). If, however, the event shape is defined for just a jet (or is simply a characteristic of the jet such as its transverse momentum), then one loses the linear dependence on soft momenta, since the question of whether one soft particle contributes to the observable is affected by its potential clustering with other soft particles.

In the case of anti-k_t jets, the independence of the jet boundary on the soft particle configuration means that the approximation eq. (6) does hold and the Milan factor retains its 'universal' value ($M = 1.49$ for 3 active non-perturbative flavours [15, 16]).

Speed. A relevant issue in order for a jet algorithm to be useful in practice is the computing time required to carry out the clustering. The full class of generalised k_t algorithms is amenable to fast implementation using the techniques of [19], with the proviso that for $p < 0$, the specific manner in which particles are clustered triggers a worst-case scenario for the Voronoi-diagram based dynamic nearest-neighbour graph determination [20]. This means that asymptotically the algorithm takes a time $\mathcal{O}\left(N^{3/2}\right)$ to cluster N particles (rather than $N \ln N$ for the k_t algorithm). However for $N \lesssim 20000$ the FastJet implementation [21] in any case uses other strategies, which are insensitive to this issue, and the anti-k_t clustering is then as fast as k_t clustering.

2.4 Example application: top reconstruction

One may wonder whether the unusual soft-resilience of the anti-k_t algorithm leads to poorer results in phenomenological applications. We have investigated various examples and found that in general this is not the case. In figure 5 we illustrate this for top mass reconstruction in LHC $t\bar{t}$ events, as simulated with Pythia [7], where both the t and the $\bar{t}$ decay hadronically, according to $t \to bW^+ \to$

[5] There are cases where, despite the added analytical complexity, this is an advantage since it can cancel a significant part of the non-global logarithms.

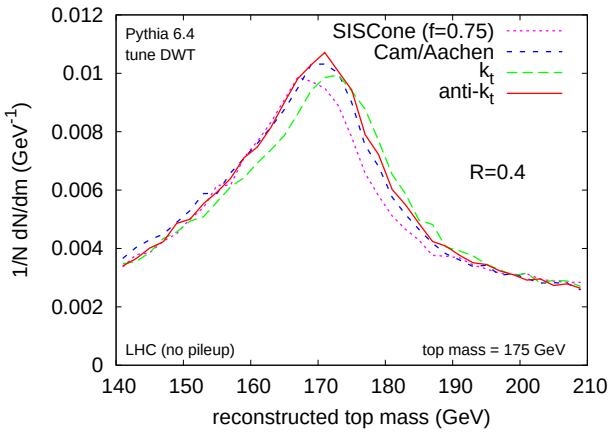

Figure 5: Top mass reconstruction in Pythia-simulated LHC $t\bar{t}$ events. Both the t and the $\bar{t}$ decay hadronically, $t \to bW^+ \to bq\bar{q}$ and $\bar{t} \to \bar{b}W^- \to \bar{b}q\bar{q}$. All jet algorithms have been used with $R = 0.4$.

$bq\bar{q}$ and $\bar{t} \to \bar{b}W^- \to \bar{b}q\bar{q}$. The following simple analysis procedure has been used: we select events with at least 6 hard jets (with p_t above 10 GeV and $|y| < 5$); we assume that both b-jets have been tagged; the 4 hardest remaining jets are paired according to the combination that better reproduces the W masses; finally, the W- and b-jets are recombined to minimise the mass-difference between the two t-jets. We use the same four algorithms shown in figure 1, now with $R = 0.4$, and find that they all behave rather similarly, with Cambridge/Aachen and anti-k_t performing marginally better than the other two. We note that the difference between various choices of R can be substantially greater than the differences between the various algorithms at a given R. One should also bear in mind that top reconstruction, near threshold, with a moderate jet radius and no pileup is a relatively simple application for inclusive jet algorithms. One expects that greater differences between algorithms will be seen in other contexts, an extreme example being multi-scale processes with large pileup.

3 Conclusions

There starts to be a certain choice of infrared and collinear safe inclusive jet algorithms for hadron colliders. As we have seen, some of these (k_t and Cambridge/Aachen) belong to a more general class of sequential recombination algorithms, parametrised by a continuous parameter p, which sets the power of the transverse momentum scale relative to the geometrical distance ($p = 1$ gives k_t, $p = 0$ gives Cambridge/Aachen).

Rather surprisingly, taking p to be negative also yields an algorithm that is infrared and collinear safe and has sensible phenomenological behaviour. We have specifically studied $p = -1$, the "anti-k_t" algorithm, and highlighted various simple theoretical properties, notably the resilience of its jet boundaries with respect to soft radiation. The other properties that we've discussed are essentially consequences of this feature. These properties are characteristic also of certain "iterative cone" (and fixed-cone) algorithms, those with progressive removal (IC-PR) of the stable cones, as used for example in CMS. However in the anti-k_t algorithm these properties are obtained without having to pay the price of collinear unsafety. Therefore the anti-k_t algorithm should be a good candidate as a replacement algorithm for IC-PR algorithms.

One might worry that the resilience (or rigidity) with respect to soft radiation could worsen

the practical performance of the tool. This seems not to be the case, at the least in examples examined so far, including the one shown in section 2.4, top reconstruction. One reason for this might be that any loss of resolution due to inflexibility in adapting to perturbative branching may be compensated for by the reduced fluctuations caused by the underlying event radiation (due to suppression of area fluctuations and back reaction). It should also be kept in mind that soft particles contribute only a modest component of the overall jet momentum, and the algorithm remains flexible in its adaptation to hard (sub)structure in the jets. In this respect it might also be interesting in future phenomenological investigations to examine less negative values of p, for which the 'hard'-adaptability extends down to softer momenta than is the case with $p = -1$.

Note. Subsequent to the first presentation of the anti-k_t algorithm and its main properties at the June 2007 Les Houches workshop on Physics at TeV colliders, it was brought to our attention by Pierre-Antoine Delsart and Peter Loch that a variant of the k_t sequential recombination algorithm had been coded within the ATLAS software framework and called reverse-k_t. It has distance measures $d_{ij} = \max(k_{ti}^2, k_{tj}^2)R^2/\Delta_{ij}^2$ and $d_{iB} = k_{ti}^2$, and recombines the pair of objects with the largest d_{ij} unless a d_{iB} is larger in which case i is called a jet. We observe that these distance measures are just the reciprocals of those for anti-k_t; together with the recombination of the most distant pair first, this causes the algorithm to produce identical jets to anti-k_t.

Acknowledgements

One of us (GPS) thanks Bruce Knuteson for a stimulating discussion on the interest of parametrised clustering jet algorithms. We are grateful to Günther Dissertori for providing us with the details of the implementation of the CMS iterative cone algorithm. Figure 5 was generated making use of tools developed in collaboration with Juan Rojo and we thank him for discussions on this and related matters. This work has been supported in part by grant ANR-05-JCJC-0046-01 from the French Agence Nationale de la Recherche and under Contract No. DE-AC02-98CH10886 with the U.S. Department of Energy.

Appendix: comment on the "iterative cone"

There are two broad classes of iterative cone algorithms: some find stables cones (of radius R) by iterating from all seeds (and sometimes midpoint seeds) and then run some split–merge procedure to deal with overlapping stable cones. These algorithms, iterative cones with a split–merge step (IC-SM), are used at the Tevatron (for instance the MidPoint algorithm) and it is our understanding that the ATLAS cone jet algorithm is of this type too. A second class takes the hardest seed particle in the event, iterates to find a stable cone, calls it a jet, removes all particles contained in that jet from the event, and then repeats the procedure with the remaining particles, over and over until there remain no seeds. This iterative-cone with progressive removal of particles (IC-PR) is the iterative cone in the CMS experiment.[6]

IC-SM algorithms have been widely studied, are known to suffer from infrared (IR) safety issues (see e.g. [3, 23, 5]). The IR safe equivalent is SISCone. Though referred to as "cones," they do not as a rule give jets with an area of πR^2 [4].

[6] It is often ascribed to UA1, ref. [22], however the algorithm described there is not based on the iteration of cones.

IC-PR algorithms have received less attention, and they behave rather differently from the IC-SM variety. For reference we therefore document some aspects of them here. A main point to note is that they suffer from a *collinear* safety issue (in the limit of a fine calorimeter). This can be illustrated with the following configuration for an algorithm with radius R:

$$p_1 : y = 0,\ \phi = 0.0R,\ p_t = 130\,\text{GeV}\,, \tag{7a}$$
$$p_2 : y = 0,\ \phi = 0.7R,\ p_t = 200\,\text{GeV}\,, \tag{7b}$$
$$p_3 : y = 0,\ \phi = 1.5R,\ p_t = 90\,\text{GeV}\,. \tag{7c}$$

The hardest seed is p_2, and in the small R limit (in which the results are independent of the recombination scheme) it leads to a jet that contains all particles, and is centred at $\phi \simeq 0.65R$. If particle p_2 splits collinearly into

$$p_{2a} : y = 0,\ \phi = 0.7R,\ p_t = 120\,\text{GeV}\,, \tag{8a}$$
$$p_{2b} : y = 0,\ \phi = 0.7R,\ p_t = 80\,\text{GeV}\,, \tag{8b}$$

then p_1 is now the hardest seed and it leads to a jet at $\phi \simeq 0.42R$ which contains p_1, p_{2a}, p_{2b}. That leaves p_3, which seeds a second jet, and so the number of hard jets is modified by the collinear splitting. This will for example lead to divergences at NNNLO in inclusive jet cross sections, at NNLO in 3-jet and W+2-jet cross sections and at NLO in jet-mass distributions for 3-jet and W+2-jet events. We recall, as discussed e.g. in [5], that a cross section that diverges at N^{p}LO can only be reliably calculated up to N^{p-2}LO. In this respect IC-PR are 'dangerous' to the same extent as midpoint-variants of the IC-SM algorithms.[7]

Unlike their IC-SM cousins, and the collinear-safety issue aside, IC-PR algorithms do have all the features of an "ideal" cone algorithm as described here for the anti-k_t algorithm, in particular they are soft-resilient and give circular jets of radius R. Thus the anti-k_t algorithm seems a natural replacement for them, especially as they happen to be identical perturbatively at NLO in the inclusive jet spectrum (if used with the same recombination scheme). An alternative replacement would be the following: find all stable cones (as in SISCone), label the hardest one a jet, remove its particles from the event, and then repeat the procedure on the remaining particles, over and over. It too would have the property of soft-resilience, but would differ perturbatively from IC-PR at NLO. This, together with the issue of computational speed, leads us to prefer the anti-k_t algorithm as a replacement.

References

[1] S. Catani, Y. L. Dokshitzer, M. H. Seymour and B. R. Webber, Nucl. Phys. B **406** (1993) 187 and refs. therein; S. D. Ellis and D. E. Soper, Phys. Rev. D **48** (1993) 3160 [hep-ph/9305266].

[2] Y. L. Dokshitzer, G. D. Leder, S. Moretti and B. R. Webber, JHEP **9708**, 001 (1997) [hep-ph/9707323]; M. Wobisch and T. Wengler, hep-ph/9907280.

[3] G. C. Blazey *et al.*, hep-ex/0005012.

[4] M. Cacciari, G. P. Salam and G. Soyez, JHEP **0804** (2008) 005 [arXiv:0802.1188].

[5] G. P. Salam and G. Soyez, JHEP **0705** (2007) 086 [arXiv:0704.0292].

[7] Note, however, that beyond LO in the inclusive jet spectrum, their perturbative expansions differ.

[6] G. L. Bayatian *et al.* [CMS Collaboration], "CMS physics: Technical design report."

[7] T. Sjostrand *et al.*, Comput. Phys. Commun. **135** (2001) 238 [hep-ph/0010017]; T. Sjostrand *et al.*, hep-ph/0308153.

[8] G. Corcella *et al.*, arXiv:hep-ph/0210213.

[9] M. Dasgupta and G. P. Salam, Phys. Lett. B **512**, 323 (2001) [arXiv:hep-ph/0104277].

[10] M. Dasgupta and G. P. Salam, JHEP **0203** (2002) 017 [arXiv:hep-ph/0203009].

[11] C. F. Berger, T. Kucs and G. Sterman, Phys. Rev. D **68** (2003) 014012 [arXiv:hep-ph/0303051].

[12] A. Banfi, G. Marchesini and G. Smye, JHEP **0208** (2002) 006 [arXiv:hep-ph/0206076].

[13] R. B. Appleby and M. H. Seymour, JHEP **0212** (2002) 063 [arXiv:hep-ph/0211426].

[14] A. Banfi and M. Dasgupta, JHEP **0401** (2004) 027 [arXiv:hep-ph/0312108]; Y. Delenda, R. Appleby, M. Dasgupta and A. Banfi, JHEP **0612** (2006) 044 [arXiv:hep-ph/0610242].

[15] Y. L. Dokshitzer, A. Lucenti, G. Marchesini and G. P. Salam, Nucl. Phys. B **511**, 396 (1998) [Erratum-ibid. B **593**, 729 (2001)] [arXiv:hep-ph/9707532]; JHEP **9805**, 003 (1998) [arXiv:hep-ph/9802381]; M. Dasgupta and B. R. Webber, JHEP **9810** (1998) 001 [arXiv:hep-ph/9809247].

[16] M. Dasgupta, L. Magnea and G. Smye, JHEP **9911** (1999) 025 [arXiv:hep-ph/9911316].

[17] M. Beneke, V. M. Braun and L. Magnea, Nucl. Phys. B **497** (1997) 297 [arXiv:hep-ph/9701309].

[18] C. Lee and G. Sterman, Phys. Rev. D **75** (2007) 014022 [arXiv:hep-ph/0611061].

[19] M. Cacciari and G. P. Salam, Phys. Lett. B **641** (2006) 57 [arXiv:hep-ph/0512210].

[20] A. Fabri *et al.*, Softw. Pract. Exper. **30** (2000) 1167; J.-D. Boissonnat *et al.*, Comp. Geom. **22** (2001) 5.

[21] M. Cacciari, G. P. Salam and G. Soyez, `http://www.lpthe.jussieu.fr/~salam/fastjet`

[22] G. Arnison *et al.* [UA1 Collaboration], Phys. Lett. B **132** (1983) 214.

[23] S. D. Ellis, J. Huston, K. Hatakeyama, P. Loch and M. Tonnesmann, Prog. Part. Nucl. Phys. **60** (2008) 484 [arXiv:0712.2447].

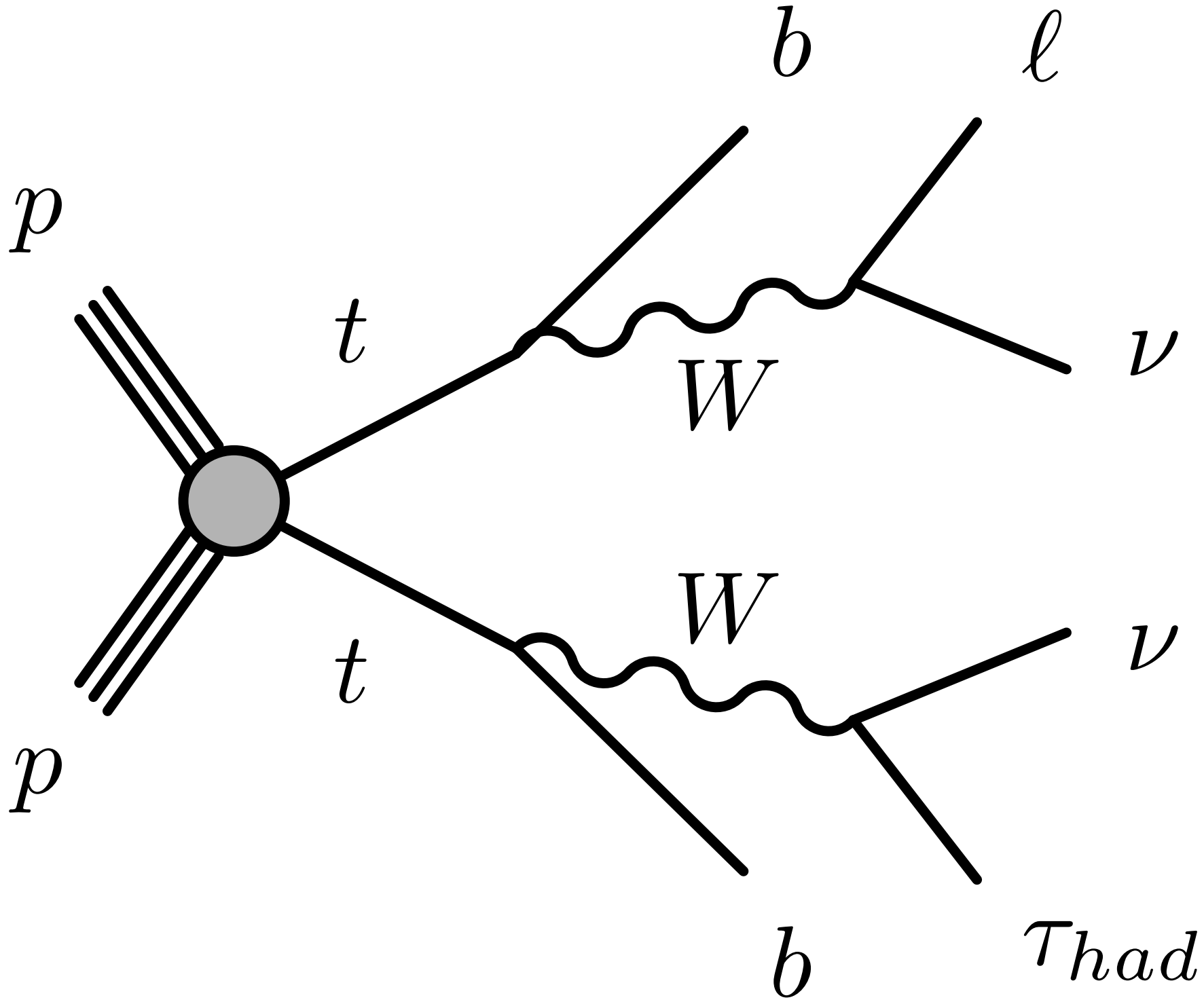
b
ℓ
p
t
W
ν
W
ν
t
p
b
τ_{had}

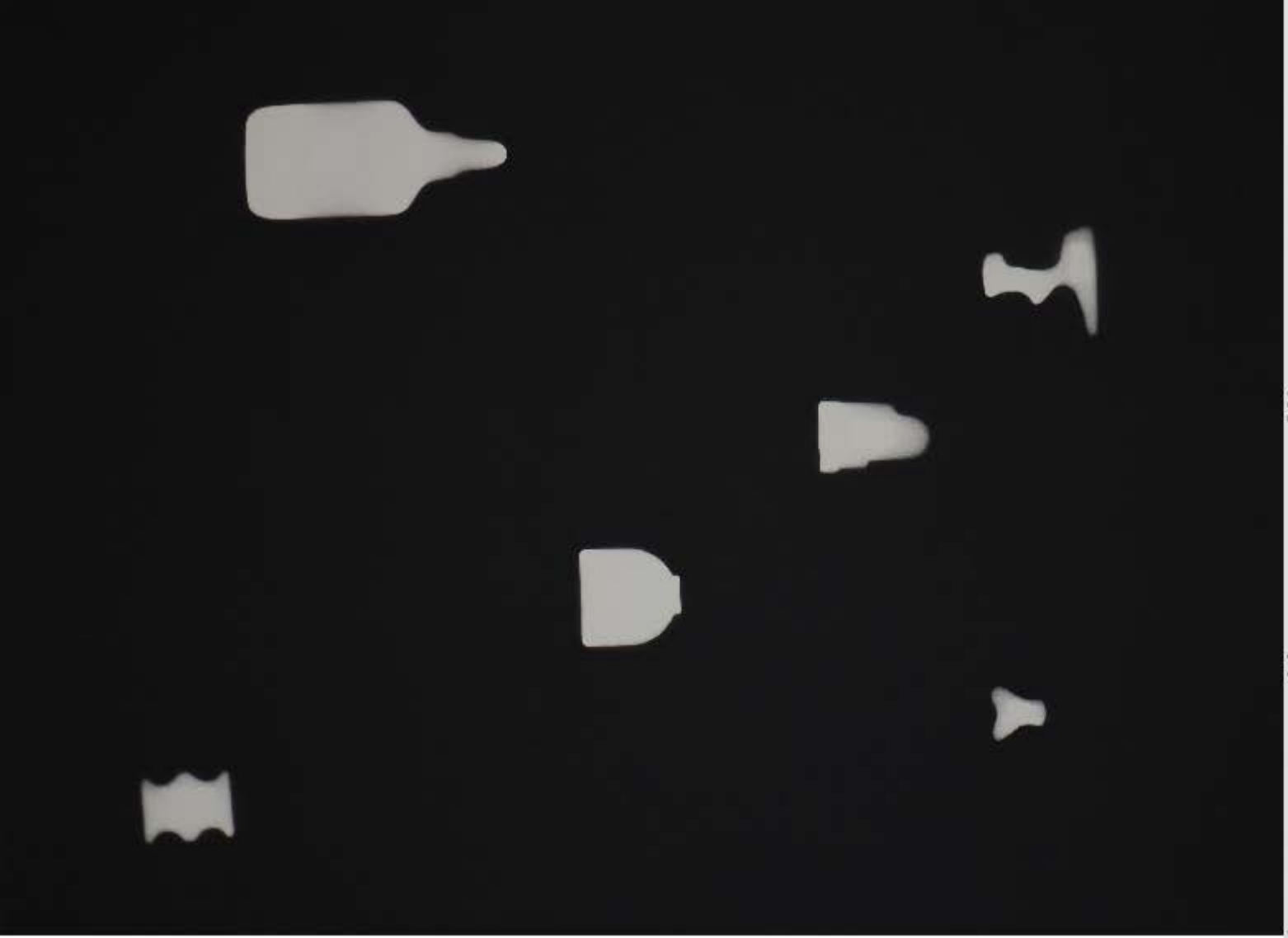

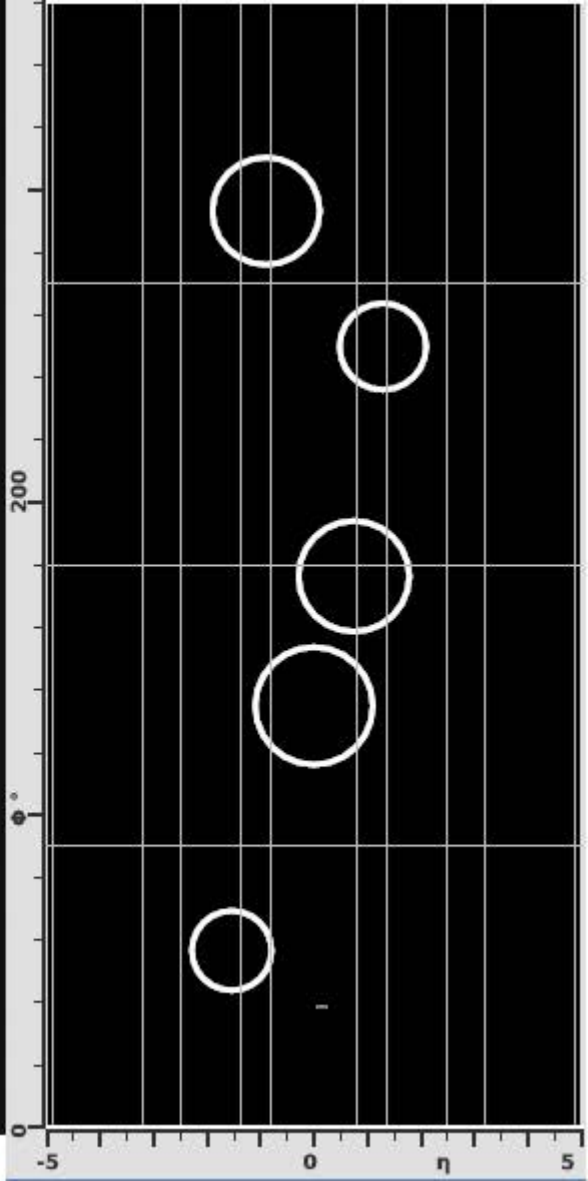
200
φ°
0
-5
0
η
5

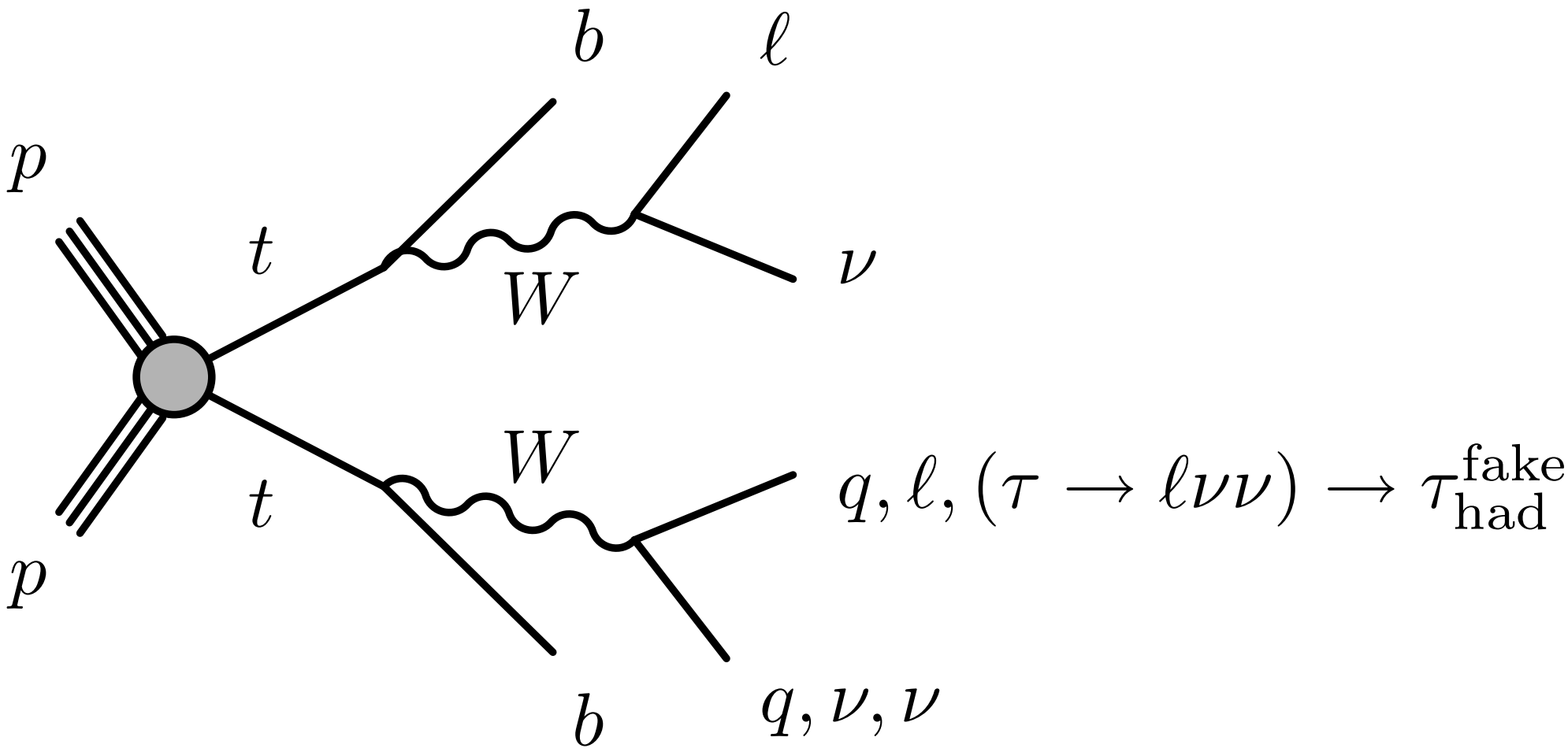
b
ℓ
p
t
W
ν
W
t
$q, \ell, (\tau \to \ell\nu\nu) \to \tau_{\mathrm{had}}^{\mathrm{fake}}$
p
b
q, ν, ν

ATLAS 2012-09-01 15:53:34 CEST run:209608 ev:94673435 lumiBlock:376 Atlantis

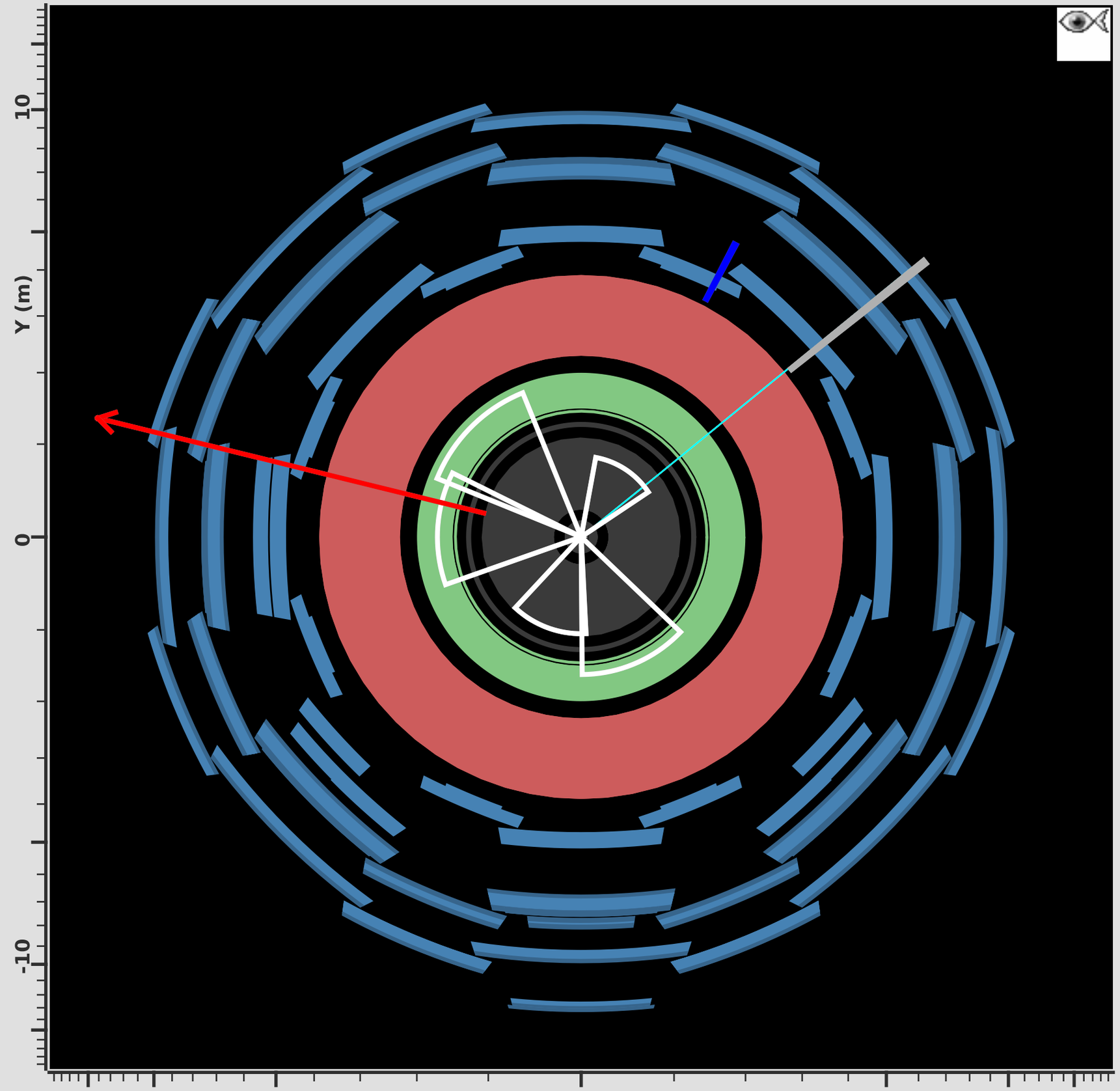

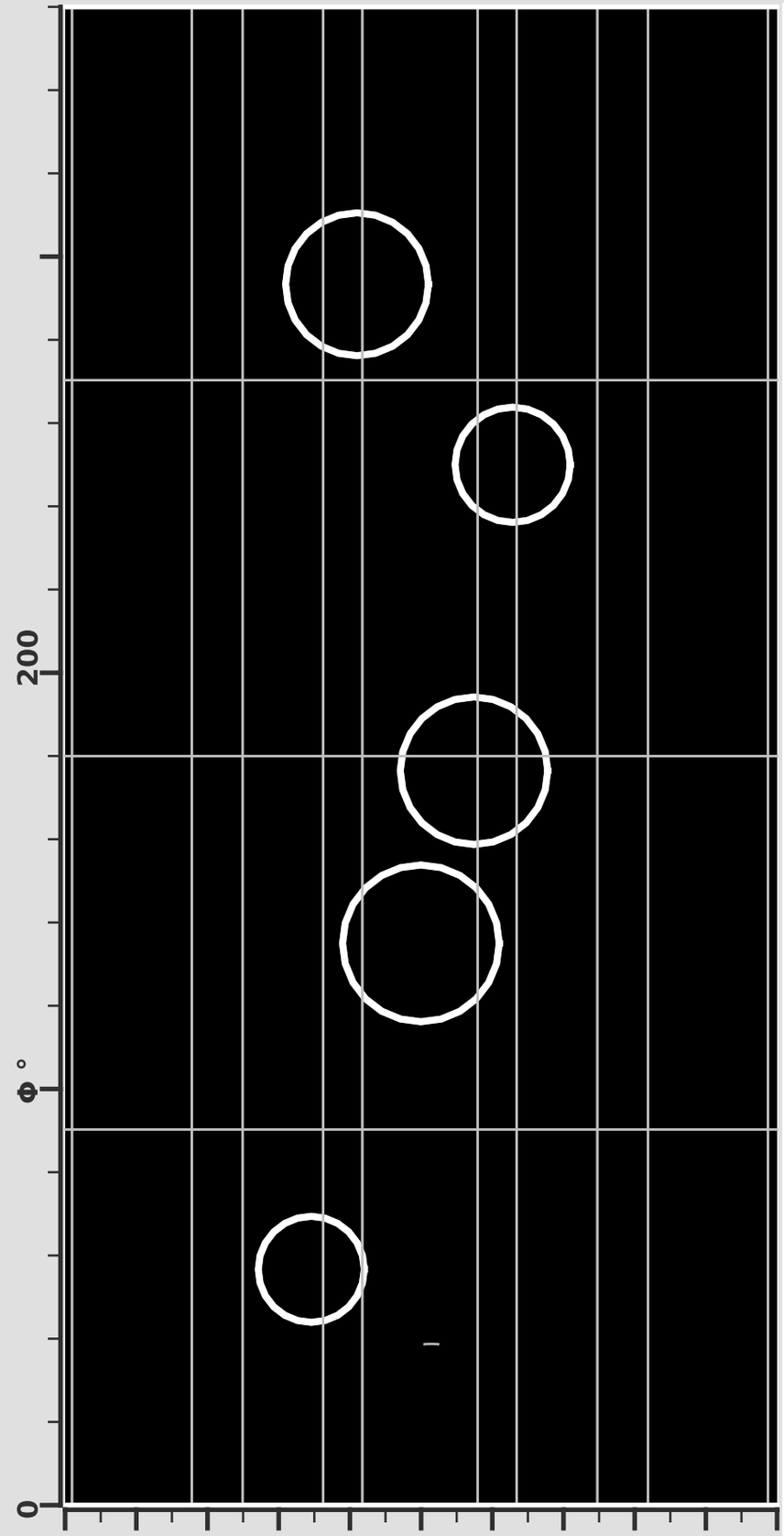

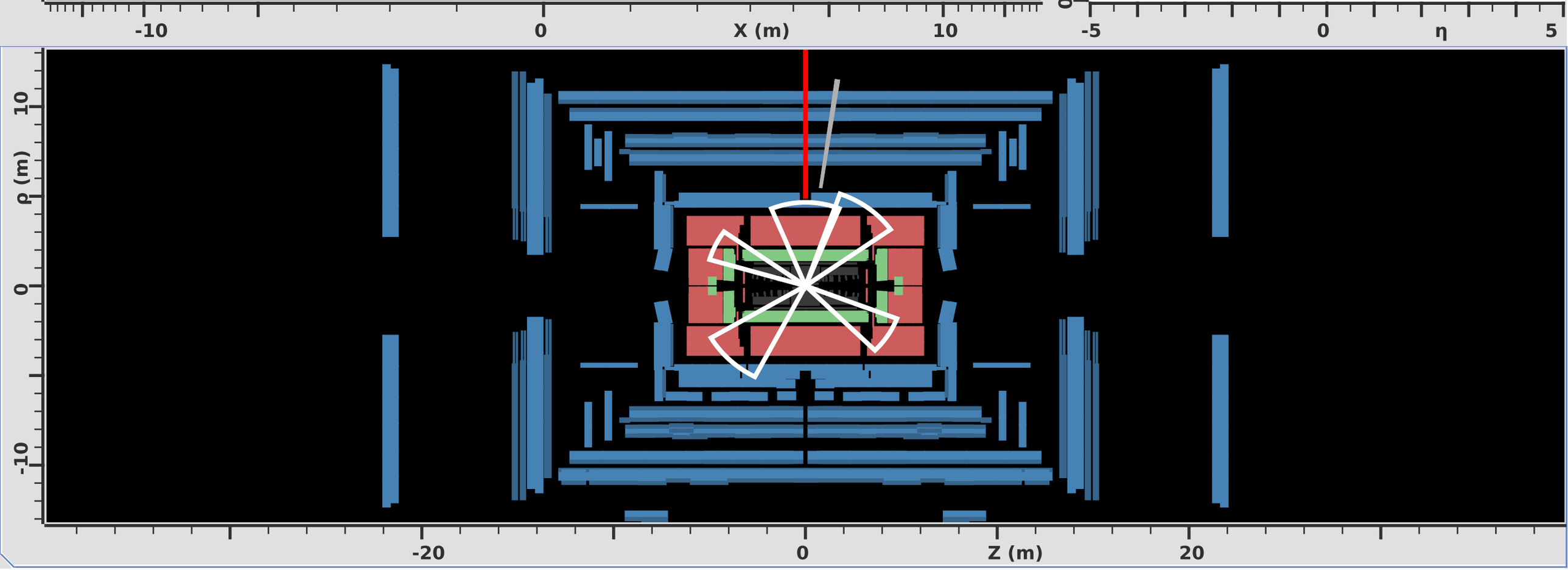

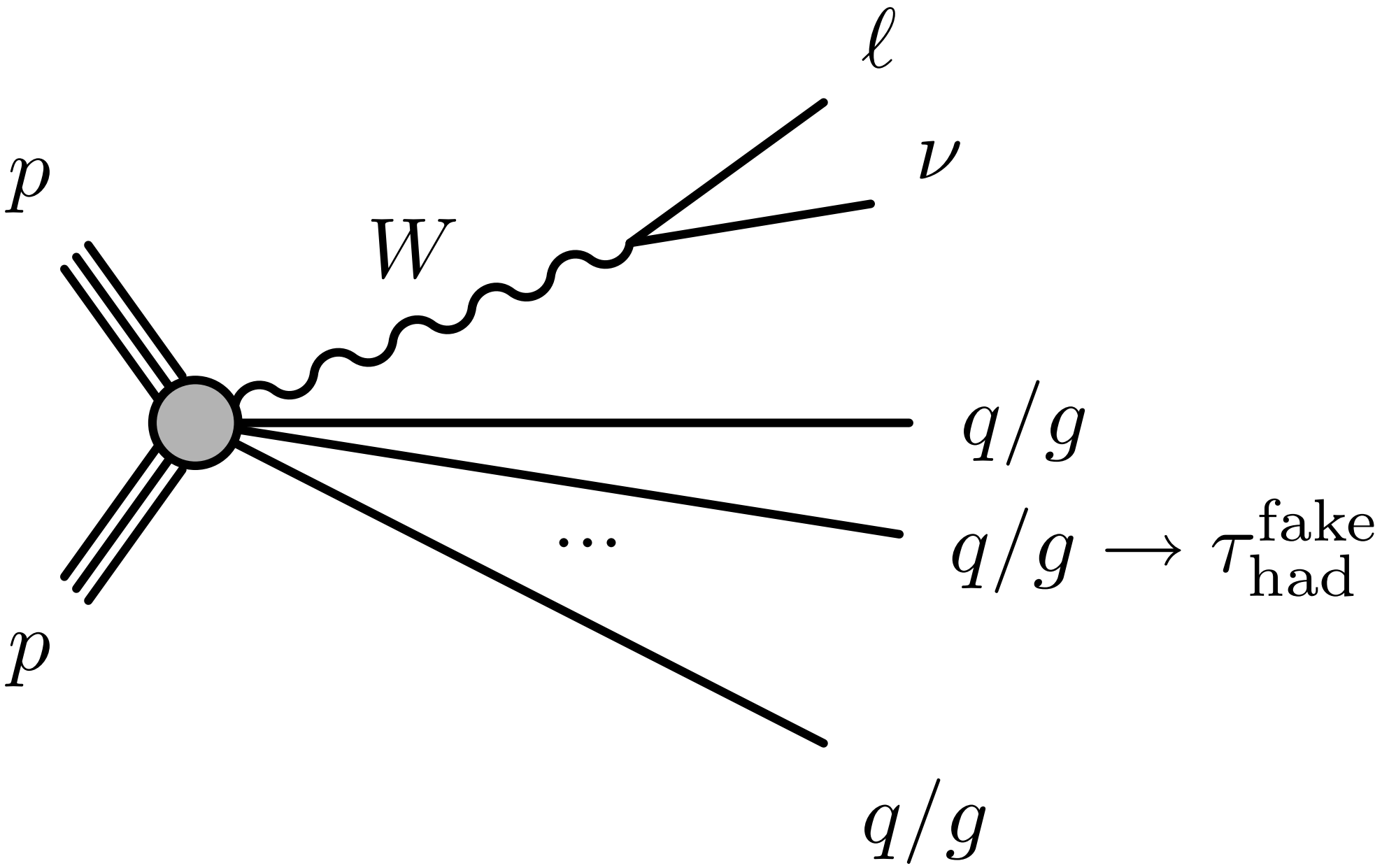
ℓ
ν
p
W
q/g
$\cdots$
$q/g \to \tau_{\mathrm{had}}^{\mathrm{fake}}$
p
q/g

Region	$N_{b-\text{jet}}$	$E_{\text{T}}^{\text{miss}}$	m_{eff}	H_{T}	$E_T^*(2E_{\text{T}}^{\text{miss}})$	$m_{\text{T2}}(\ell, \tau_{\text{had}})$	$m_{\text{T}}(\ell, p_{\text{T}}^{\text{miss}})$
SR	≥ 0	> 150 GeV	> 350 GeV	> 100 GeV	> 180 GeV	> 120 GeV	> 100 GeV
CRTt	≥ 1	> 150 GeV	> 350 GeV	> 100 GeV	> 180 GeV	20-80 GeV	> 120 GeV
CRTf	≥ 1	> 150 GeV	> 350 GeV	> 100 GeV	> 180 GeV	20-80 GeV	< 120 GeV
CRW	0	> 150 GeV	> 350 GeV	> 100 GeV	> 180 GeV	20-80 GeV	40-100 GeV
VRmet	≥ 0	< 150 GeV	> 350 GeV	> 100 GeV	> 180 GeV	> 80 GeV	> 100 GeV
VRmt	≥ 0	> 150 GeV	> 350 GeV	> 100 GeV	> 180 GeV	> 80 GeV	< 100 GeV

Reading the figures left to right and top to bottom (like a book) from the original piece of art:

mini bike seat turned into a muon
laser gun turned into a jet
padlock turned into a jet
flat vase turned into a jet
glue bottle turned into a jet
fighter ship turned into a hadronically decaying tau

The assymetry in the heights of the painted objects distributed in the phi direction creates Missing Transverse Momentum, which is assumed to come from undetected particles.